Characteristics of tin oxide nanoparticles produced by pulsed laser ablation technique in various concentrations of chitosan liquid and their potential application as an antibacterial agent

by Iis Nurhasanah

Results in Engineering 16 (2022) 100742

Contents lists available at ScienceDirect

Results in Engineering

journal homepage: www.sciencedirect.com/journal/results-in-engineering

Characteristics of tin oxide nanoparticles produced by pulsed laser ablation technique in various concentrations of chitosan liquid and their potential application as an antibacterial agent

Ali Khumaeni [a,b,*], Tri Istanti [a], Eko Hidayanto [a], Iis Nurhasanah [a]

[a] *Department of Physics, Faculty of Science and Mathematics, Diponegoro University, Jl. Prof. Soedharto, SH., Tembalang, 50275, Semarang, Indonesia*
[b] *Research Center for Laser and Advanced Nanotechnology, Faculty of Science and Mathematics, Diponegoro University, Jl. Prof. Soedharto, SH., Tembalang, 50275, Semarang, Indonesia*

ARTICLE INFO

Keywords:
Tin oxide nanoparticles
Pulse laser ablation
Nd:YAG laser
Chitosan medium

ABSTRACT

Tin oxide nanoparticles (SnO_2 NPs) have become a potential candidate as an antibacterial agent for gram-negative and gram-positive bacteria. In this present work, SnO_2 NPs have been successfully synthesized in the chitosan liquid medium by using the pulse laser ablation method utilizing quite low energy Nd:YAG laser (30 mJ). The produced tin oxide nanoparticles were then applied as an antibacterial agent for gram-negative and gram-positive bacteria. Experimentally, a pulse Nd:YAG laser beam is irradiated and focused on the surface of a high-purity tin metal plate placed at the bottom of the Petri dish that is filled with chitosan liquid medium. The effect of chitosan concentrations (0.05%, 0.1%, and 0.2%) on the characteristics of produced SnO_2 NPs was examined. The higher concentration of chitosan (0.2%) gains the smallest diameter size (15.05 nm) and lowest concentrations of produced tin oxide nanoparticles. The application of produced SnO_2 NPs as the antibacterial agent was demonstrated using gram-negative (*Escherichia coli*) and gram-positive (Bacillus subtilis) utilizing disk diffusion technique. The result certified that increment of the SnO_2 NPs concentrations (100, 125, and 150 ppm) increases the diameter of inhibition zone (DIZ) both for E coli and B subtilis bacteria, which approve that the produced tin oxide nanoparticles can effectively be used as antibacterial agents for both gram-negative and gram-positive bacteria.

1. Introduction

Nanotechnology has now become an emerging subject embraced by many sectors including science and industries [1–6]. In industries, nanotechnology has started to be applied in energy technology, food technology, environmental technology, and medical products [7–12]. As medical products, nanotechnology has been used in the diagnosis and treatment of diseases.

In the medical field, infections of bacteria are major chronic infections and can cause a worse case of mortality. One of the treatments for such an infection is using antibiotics. However, based on many studies [13–15], the use of antibiotics can cause bacterial strains of drug-resistant. To avoid this problem, nanoparticles are recently used because the NPs is in direct contact with the cell wall of bacteria, without any need to penetrate the cell, resulting in less prone to promoting resistance in bacteria. Various metallic nanoparticles have been produced for being used as an antibacterial agent including zinc nanoparticles, titanium oxide nanoparticles, silver nanoparticles, gold nanoparticles, copper oxide nanoparticles, and tin nanoparticles [16–22].

Tin oxide nanoparticles (SnO_2) have recently been widely produced for various applications including antibacterial agents [23–25]. The tin oxide nanoparticles have been manufactured using various techniques such as precipitation, hydrothermal, chemical reduction, hydrolysis, and sol-gel methods [26–32]. Ibarguen et al. produced tin oxide nanoparticles using a precipitation technique [30]. Some researchers used the sol-gel method to produce tin oxide nanoparticles [31]. The methods can be used to produce stable colloidal tin oxide nanoparticles with quite a good size distribution of nanoparticles. However, the methods have several drawbacks including complicated experimental preparation and requiring additional chemical agents such as chemical acid and chemical surfactants. Furthermore, the described methods also cannot produce

* Corresponding author.
E-mail address: khumaeni@fisika.fsm.undip.ac.id (A. Khumaeni).

https://doi.org/10.1016/j.rineng.2022.100742
Received 8 September 2022; Received in revised form 17 October 2022; Accepted 28 October 2022
Available online 7 November 2022

high-purity colloidal nanoparticles due to the contamination of chemical agents added during the synthesis process [33,34].

The other technique used is the physical method of pulse laser ablation in liquid media [35]. In this technique, a pulse laser including pulse nano- and femto-second lasers such as Nd:YAG laser and Ti: Sapphire laser is commonly used as an energy source to ablate material and induce a luminous plasma [36,37]. The plasma is then condensed in the liquid media and finally produced nanoparticles dispersed in the liquid media. Some papers have reported the production of tin nanoparticles using a pulse laser ablation method [38,39]. Gondal et al. synthesized tin oxide nanoparticles by an Nd:YAG laser ablation in deionized water and their photoluminescence characteristics [38].

In this present work, we used a chitosan liquid as an organic surfactant in the production of tin oxide nanoparticles using the pulse laser ablation method utilizing pulse Nd:YAG laser. Chitosan liquid medium with various solution concentrations was used in the synthesis of tin oxide nanoparticles (SnO_2 NPs). Chitosan is a natural polymer that can be easily isolated from crustacean shells and is considered a non-toxic, odorless, biocompatible, and biodegradable biopolymer [40,41]. In the formation of nanoparticles, chitosan can act as a stabilizer, reducing agent, sizing agent, and shape-directing agent for the synthesis of metal nanoparticles [42,43]. The effect of chitosan concentrations on the characteristics of produced tin oxide nanoparticles is studied. Further, the produced nanoparticles are applied as an antibacterial agent using E coli and B subtilis bacteria.

2. Experimental procedures

The basic experimental setup used in this present work is shown in Fig. 1. A pulse neodymium yttrium aluminum garnet (Nd:YAG laser, New Wave Polaris II, 1064 nm, 50 mJ, 7 ns) was used as a material ablation source. A pulse laser beam was focused by a quartz lens with a focal length of 30 mm on a metal plate, which was placed and immersed in a liquid medium, to induce a luminous plume. The laser energy was set at 30 mJ and a repetition rate of 10 Hz. Using those parameters, the laser beam diameter at the focusing point on the surface was 80 μm, resulting in the laser fluence on the sample surface of 8.5 GW/cm^2.

The metal sample used to produce tin oxide nanoparticles was high-purity tin metal nanoparticles (Nilaco Inc., 99.99%). In the experiments, the tin metal was immersed in a chitosan solution, which functions as a surfactant to keep the stability of the produced nanoparticles. After several shots of laser bombardment, the luminous plume was induced just on the surface of the metal plate and finally, the tin oxide nanoparticles were produced and dispersed in the liquid to produce colloidal tin oxide nanoparticles.

The produced tin oxide nanoparticles were then characterized by using analytical and spectroscopic methods including transmission electron microscopy (TEM, JEOL JEM 1400), scanning electron microscopy-the energy dispersive X-ray (EDX, JEOL JSM-6510LA SEM-EDX), ultraviolet–visible light spectroscopy (UV–Vis, Merck's Pharo 300 Spectroquant Spectrophotometer), and Fourier Transform Infra-Red (FTIR) Spectrophotometer (FTIR PerkinElmer Spectrum Version 10.4.00). It should be informed that the TEM was used to obtain morphological characteristics of tin oxide nanoparticles. The EDX was employed to get the analytical composition of produced nanoparticles. The UV–Vis and FTIR were used to determine the optical characteristics of the absorbance spectrum and were also carried out to identify functional groups and compounds contained in tin oxide nanoparticles.

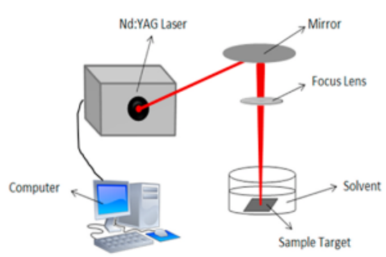

Fig. 1. Experimental setup used in this work.

Finally, the produced tin oxide nanoparticles were examined as an antibacterial agent by testing the nanoparticles using the disc diffusion technique. The samples contain various concentrations of tin oxide nanoparticles of 100 ppm, 125 ppm, and 150 ppm, respectively. Two kinds of bacteria were employed including *Escherichia coli* and Bacillus subtilis. The disc diffusion technique was made by measuring the diameter of the inhibition zone (DIZ), which is an indication of an inhibitory response to bacterial growth by the antibacterial compound in the extract. The bacterial suspension was diluted to have a turbidity level or optical density of 0.5 Mc Farland. The standard of 0.5 Mc Farland is the number of bacteria in 1 mL of suspension estimated at 1.5 × 10^8 bacteria. The test medium was made by mixing the agar nutrients with a diluted suspension of *Escherichia coli* bacteria. The media was stirred until evenly distributed and then allowed to dry and solidify (plate medium). Furthermore, the filter paper that has been sterilized was then immersed in each colloidal SnNPs with various concentrations of 100 ppm, 125 ppm, and 150 ppm. The filter paper was then placed on the test media. The test media was put into an incubator at 37 °C for 18–24 h and the inhibition zone diameter was observed.

3. Results and discussion

First, the effect of various concentrations of chitosan liquid medium was studied in the production of tin oxide nanoparticles. Figs. 2–4 show the colloidal tin oxide nanoparticles produced in the chitosan liquid media with chitosan concentrations of 0.05%, 0.1%, and 0.2%, respectively. It should be noted that in the case of chitosan concentration beyond 0.2%, the chitosan liquid is too thick. Therefore, when the pulse laser beam is directed and focused on the tin metal plate via chitosan liquid, lots of laser beams are absorbed by the liquid, resulting in small plasma produced on the metal surface due to low laser energy remaining attacked on the metal plate. Before laser bombardment, chitosan liquid media have transparent color as displayed in Figs. 2(a), 3(a) and 4(a). The brownish-yellow color colloidal nanoparticles are successfully produced in all samples just after laser bombardment on the high-purity tin metal plate as shown in Figs. 2(b), 3(b) and 4(b). That colloidal color is almost similar to the colloids produced by Naser et al. and Ismail et al., which produced colloidal tin nanoparticles in various liquid media that have a brownish color [44,45]. After 1 day of being synthesized, the colloidal still keeps the same color even though the cloudy white color starts to produce in the bottom of the bottle. These cloudy white color particles are produced by the agglomeration of tin oxide nanoparticles dispersed in the chitosan liquid medium. Nanoparticles dispersed in the

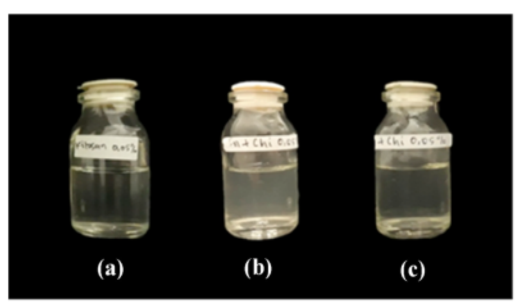

Fig. 2. Photographs of colloidal tin oxide nanoparticles in chitosan liquid medium with a concentration of 0.05% (a) chitosan liquid only before laser bombardment, (b) just after laser bombardment, and (c) 2 days after laser bombardment.

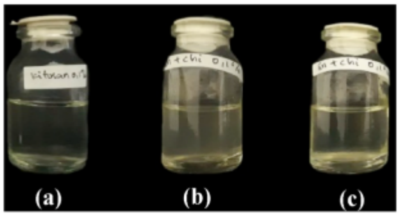

Fig. 3. Photographs of colloidal tin oxide nanoparticles in chitosan liquid medium with a concentration of 0.1% (a) chitosan liquid only before laser bombardment, (b) just after laser bombardment, and (c) 2 days after laser bombardment.

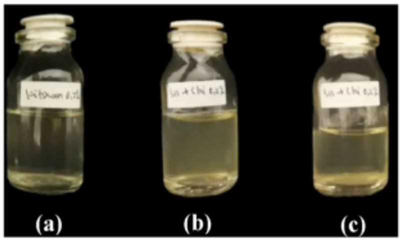

Fig. 4. Photographs of colloidal tin oxide nanoparticles in chitosan liquid medium with a concentration of 0.2% (a) chitosan liquid only before laser bombardment, (b) just after laser bombardment, and (c) 2 days after laser bombardment.

liquid phase adhere to each other and spontaneously form a collection of irregular particles such as floc clusters or aggregates, the aggregates form agglomerates of larger particles which is one of the causes of colloid destabilization [46]. Much more cloudy white fine particles are produced in the bottom after 2 days of nano synthesis as displayed in Figs. 2(c), 3(c) and 4(c), respectively. However, it should be noticed that much fewer cloudy white fine particles are observed in the case of chitosan solution with a concentration of 0.2%. This result certified that the highest concentration of chitosan can produce much more stable colloidal tin oxide nanoparticles; the cloudy white fine particles are the tin oxide particles produced due to the agglomeration of the dispersed tin oxide nanoparticles because the chitosan surfactant cannot work well to retard the combination of tin oxide nanoparticles. Based on these results, chitosan concentrations of 0.2% can produce much more stable tin oxide nanoparticles.

The produced tin oxide nanoparticles are then characterized by using some analytical and imaging spectroscopic methods. First, their morphological characteristics are examined. Fig. 5 shows the TEM images obtained from the colloidal tin oxide nanoparticles in chitosan liquid media containing various concentrations of chitosan.

It can be seen that the shape of the produced tin nanoparticles has the same spherical shape for the case of 0.05%, 0.1%, and 0.2% chitosan media as displayed in Fig. 5(a), (b), and 5(c), respectively. These spherical shapes of nanoparticles are commonly produced for the case of metal nanoparticles synthesized by using the pulse laser ablation method as shown in some papers [47–49]. It should also be noted that the number of produced spherical nanoparticles of tin oxide is more agglomerated for the lowest concentrations of 0.05% chitosan medium (Fig. 5(a)) compared to the 0.1% and 0.2% cases as displayed in Fig. 5(b) and (c). Tin nanoparticles produced by the pulse laser ablation in a liquid medium are easily oxidized to form tin oxide nanoparticles [50]. The tin oxide nanoparticles are readily agglomerated when being produced in the liquid medium [51]. Therefore, surfactants or stabilizer chemical agents are commonly used to avoid agglomeration to produce stable colloidal metal nanoparticles. However, the thin concentration of

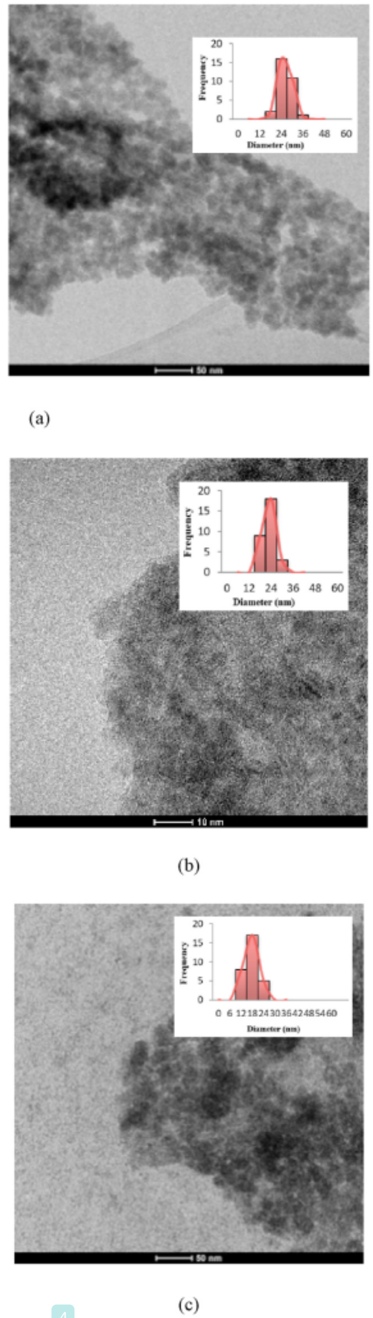

Fig. 5. TEM images of tin oxide nanoparticles in the chitosan liquid medium with a concentration of (a) 0.05%, (b), 0.1%, and (c) 0.2%.

chitosan medium (0.05%) is still not enough to stabilize the produced nanoparticles, resulting in more agglomeration of nanoparticles each-others. Therefore, a quite thick concentration of chitosan (0.2%) is more effective to produce stable colloidal tin oxide nanoparticles as shown in Fig. 5(c). By using the particle size analyzer technique, the produced nanoparticles are estimated in their sizes as shown in the insert of Fig. 5(a), (b), and 5(c). It is seen that the averaged diameter of produced nanoparticles in various chitosan mediums are 22.76 nm, 20.13 nm, and 15.05 nm for the case of 0.05%, 0.1%, and 0.2%, respectively. The same result on the effect of surfactant concentration on the morphological characteristics of produced nanoparticles is also obtained as reported in this previous paper [52]. The difference in the averaged nanoparticle diameters was obtained from the effect of using variations in the concentration of chitosan liquid medium. Variations in the concentration of chitosan liquid medium from 0.05%, 0.1%, 0.2% affect the Brownian motion between the nanoparticles produced. Brownian motion is the random motion of nanoparticles caused by the collision of nanoparticles with each other [53].

Insert of Fig. 5. Diameter size distribution of tin oxide nanoparticles in the chitosan liquid medium with a concentration of (a) 0.05%, (b), 0.1%, and (c) 0.2%.

In the synthesis of tin oxide nanoparticles with a stabilizer and without a stabilizer, the results of the nanoparticles are more agglomerated in the synthesis of SnO_2 NPs without a stabilizer. These clumps occur as a result of Brownian motion in a medium without a stabilizer moving faster, nanoparticles are difficult to distinguish from one another so the tendency to agglomerate (agglomeration) increases [54]. Concentration of 0.05% and 0.1% have lower stabilizer content than 0.2% concentration. At a concentration of 0.05% and a concentration of 0.1% with a lower level of stabilizer content, it produces a more agglomerated image with a tendency to be difficult to distinguish between nanoparticles, thereby increasing the chance of agglomeration. Based on this result, it is obtained that the tin oxide nanoparticles produced in the chitosan liquid medium with a concentration of 0.2% can produce a much smaller size and more stable tin oxide nanoparticles.

The optical characteristic of produced tin oxide nanoparticles is characterized by UV–Vis spectroscopy as shown in Fig. 6. The absorbance spectra are obtained from the tin oxide nanoparticles produced in various concentrations of chitosan liquid media with the same duration of ablation and repetition rate of synthesis. As seen in the figure that the highest absorbance intensity is obtained from the tin oxide nanoparticles produced in 0.05% chitosan, while the lower intensities are gained from the 0.1 and 0.2% chitosan, respectively. This is because in the case of the highest concentration of chitosan liquid medium (0.2%), the laser energy absorbed by the chitosan medium before hitting the Sn metal target is much higher than the case of lowest concentration 0.05% chitosan, and therefore the laser energy attacking the Sn material target is much lower for the case of the highest concentration chitosan, resulting in much fewer ablated particles. Furthermore, in the case of the highest concentration chitosan, the ablated tin nanoparticles being agglomerated are less so that the particle density in the chitosan solution is reduced, resulting in lower maximum absorption than the case of lowest concentration chitosan. As seen in the figure, the maximum wavelength for the case of 0.05% chitosan is 240 nm. With increasing the concentrations of chitosan, the maximum wavelengths shift to the lower wavelengths; namely, 232 nm and 223 nm, respectively, for 0.1% and 0.2% chitosan concentrations. This result is also confirmed by Muñoz et al. that the increasing of the nanoparticle diameter results in a longer maximum wavelength in agreement with Mie's theory [55].

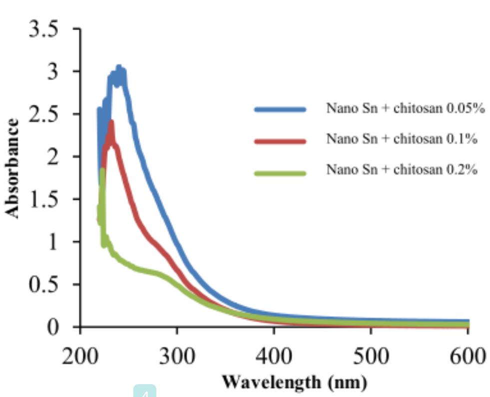

Fig. 6. UV–Vis spectra of tin oxide nanoparticles in the chitosan liquid medium with a concentration of 0.05%, 0.1%, and 0.2%.

The other characteristics examined in this present work are analytical characteristics of produced colloidal tin oxide nanoparticles. Fig. 7 shows the EDX spectrum obtained from the tin oxide nanoparticles produced by using the pulse ablation method in a chitosan liquid medium. It can be seen that the analytical lines of Sn, O, C, and Si occur with quite high intensity. The C and Si that appeared in this spectrum might come from the SiC material used as a substrate for the deposition of the tin oxide nanoparticles during data acquisition. Sn line has the highest intensity compared to other analytical lines. The Sn and O lines are contributed from the tin oxide nanoparticles produced in this present work. These analytical lines confirmed that the tin oxide nanoparticles have been successfully produced by using our pulse laser ablation technique. Furthermore, the result confirmed that the colloidal tin oxide nanoparticles produced by using the present laser ablation technique have high purity because there are no other elements and only Sn, O, C, and Si are detected in the spectrum.

To know the functional groups of tin oxide nanoparticles, Fourier transform infrared spectroscopy (FTIR) was applied. Fig. 8 displays the FTIR spectrum obtained from the tin oxide nanoparticles. Four functional groups are identified from the spectrum including O–H, C=C, C–N, and Sn–O. From the spectrum, we obtained that the O–H appears at 3391.01 cm^{-1}, C=C, C–N, and Sn–O occur at 1643.37, 1178.56, and 629.03 cm^{-1}, respectively. The occurrence of Sn–O in the spectrum stated that the functional SnO_2 has been produced during the synthesis process. Those functional groups have similar results obtained in the previous work on the synthesis of tin oxide nanoparticles [56].

Fig. 9 shows the XRD spectrum obtained from the tin oxide nanoparticles produce in Chitosan liquid with a concentration of 0.1%. The products' diffraction spectrum and inter-plane spacing matched the typical diffraction pattern of SnO_2, supporting the synthesis of SnO_2 nanocrystals and suggesting that ablated Sn species were present. The main peak of SnO_2 was obtained at $2\theta = 26.67^o$, which corresponds to (110). This result indicated that crystalline tin oxide nanoparticles are produced in this present work.

Finally, the produced tin oxide nanoparticles are examined as an antibacterial agent using two bacteria as representative of gram-negative and gram-positive bacteria of *Escherichia coli* and Bacillus subtilis, respectively. The test was made using the disk diffusion method by considering the inhibition zone diameter (DIZ) as reported in previous papers. The DIZ value reflects the magnitude of the susceptibility of microorganisms to certain antibacterial agents, and the size of the DIZ strain that is susceptible to disinfectants is larger than the resistant strain [57]. The samples used include positive control and our produced tin oxide nanoparticles with various concentrations of 100 ppm, 125 ppm,

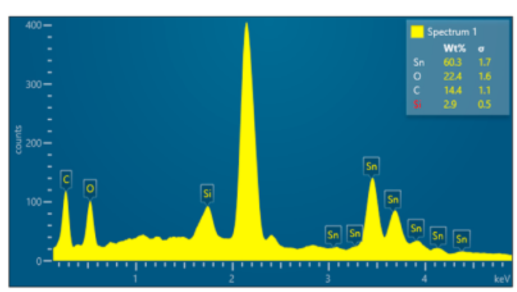

Fig. 7. EDX emission spectrum obtained from the tin oxide nanoparticles in 0.1% chitosan liquid medium.

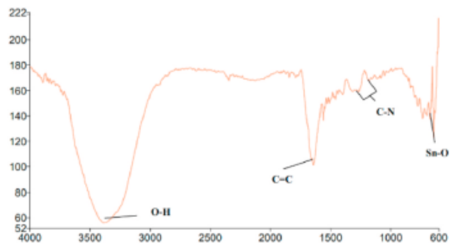

Fig. 8. FTIR spectrum obtained from the tin oxide nanoparticles in 0.1% chitosan liquid medium.

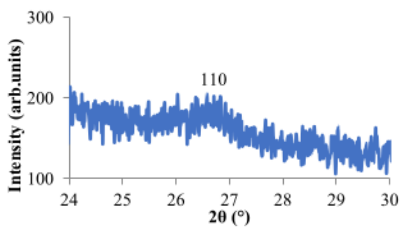

Fig. 9. XRD spectrum obtained from the tin oxide nanoparticles in 0.1% chitosan liquid medium.

and 150 ppm. As a positive control, the Terramycin sample, an antibiotic that contains an antimicrobial effect, is used. This sample is generally used to treat infections by gram-positive and gram-negative bacteria. The result of the antibacterial examination is shown in Table 1.

Positive control of Terramycin shows a good effect as an antibacterial agent both for gram-negative (E coli) bacteria and gram-positive (B subtilis) bacteria with DIZ values for both bacteria of 15.38 and 14.89 mm, respectively, which demonstrated that there is the prohibition of bacterial activity in the phase of death. The produced tin oxide nanoparticles were then examined at various concentrations. The results show that the concentrations of 100 ppm, 125 ppm, and 150 ppm result in DIZ values of 7.74 mm, 7.52 mm, and 9.49 mm, respectively, for the E coli bacteria (gram-negative bacteria), while the DIZ values are 6.71 mm, 8.30 mm, and 8.74 mm, respectively, for the case of B subtilis (gram-positive bacteria). With increasing the concentration of the tin oxide nanoparticles, the diameter of the inhibition zone increases, which means that the inhibition of bacterial activity increases. This similar tendency is also reported in the previous papers [58]. This condition can be explained when the concentration of SnO_2 nanoparticles increases, so that more nanoparticles are absorbed into bacterial cells so that the dehydrogenation process of bacterial cells also increases. Dehydrogenation occurs due to the process of respiration that occurs in the bacterial cell membrane. After reacting with the nanoparticles, the bacteria begin to deactivate their enzymes, producing hydrogen peroxide which causes bacterial cell death [59]. This result confirmed that the tin oxide nanoparticles produced in this present work can be employed as an antibacterial agent both for gram-negative and gram-positive bacteria such as E coli and B subtilis, respectively.

4. Conclusions

Synthesis of tin oxide nanoparticles in chitosan liquid medium has been successfully conducted using pulse laser ablation technique utilizing pulse Nd:YAG laser with laser energy of around 30 mJ. The effect of chitosan concentrations (0.05%, 0.1%, and 0.2%) in the chitosan medium on the characteristics of produced tin oxide nanoparticles was examined, resulting in the smallest diameter size of nanoparticles (15.05 nm) for the highest concentration of chitosan (0.2%) and the highest produced tin oxide nanoparticles in the lowest chitosan concentration (0.05%). The produced tin oxide nanoparticles have antibacterial characteristics demonstrated by examination of the nanoparticles as an antibacterial agent of gram-negative (E coli) and gram-positive (B subtilis). The results show that the higher concentrations of tin oxide nanoparticles increase the inhibition zone of bacterial activity for *E. coli* and B. subtilis bacteria shown by the largest DIZ value for the highest concentrations case. This result demonstrated that the produced tin oxide nanoparticles are applicable as an antibacterial agent both for gram-negative and gram-positive bacteria.

Table 1
Antibacterial test of tin oxide nanoparticles at various concentrations using disk diffusion technique.

Sample	DIZ (mm)	Bacteria
100 ppm	7,74	*Escherichia coli*
125 ppm	7,52	
150 ppm	9,49	
Positive control	15,38	
100 ppm	6,71	Bacillus subtilis
125 ppm	8,30	
150 ppm	8,74	
Positive control	14,89	

Credit author statement

Ali Khumaeni: Ideas and design methodology, analysing the experimental results, Tri Istanti: Conducting a research and data collection, Eko hidayanto: Provision of materials, analysing the experimental results, Iis Nurhasanah: Antibacterial applications and analysing the experimental results.

Declaration of competing interest

The authors declare that they have no known competing financial interests or personal relationships that could have appeared to influence the work reported in this paper.

Data availability

Data will be made available on request.

Acknowledgments

This work was financially supported by Diponegoro University Indonesia under Research Grant for International Publication No.233–24/UN7.6.1/PP/2021. Part of this work was also financially supported by Matching Fund 2022.

References

[1] S. Rai, A. Rei, Nusantara Biosci. Rev. 7 (2015) 2, https://doi.org/10.13057/nusbiosci/n070201.
[2] V. Amenta, K. Aschberger, M. Arena, H. Bouwmeester, F.B. Moniz, P. Brandhoff, S. Gottardo, H.J.P. Marvin, A. Mech, L.Q. Pesudo, H. Rauscher, R. Schoonjansc, M. V. Vettoric, S. Weigel, R.J. Peters, Regul. Toxicol. Pharmacol. 73 (2015) 1, https://doi.org/10.1016/j.yrtph.2015.06.016.
[3] S.M. Solaiman, Y. Yamauchi, J.H. Kim, J. Horvat, S.X. Dou, G. Alici, L. Ooi, B. Martinac, M.J.A. Shiddiky, V. Gopalan, M.S.A. Hossain, Nanotechnol. Rev. 6 (2017) 3, https://doi.org/10.1515/ntrev-2016-0095.
[4] X. He, H.-M. Hwang, J. Food Drug Anal. 24 (2016) 4, https://doi.org/10.1016/j.jfda.2016.06.001.
[5] W. Hannah, P.B. Thompson, J. Environ. Monit. 3 (2008), https://doi.org/10.1039/B718127M.
[6] B.G. Priestly, A.J. Harford, M.R. Sim, MJA (Med. J. Aust.) 186 (2007) 4, https://doi.org/10.5694/j.1326-5377.2007.tb00859.x.
[7] T. Singh, S. Shukla, P. Kumar, V. Wahla, V.K. Bajpai, I.A. Rather, Front. Microbiol. 8 (2017) 1501, https://doi.org/10.3389/fmicb.2017.01501.
[8] R. Ravichandran, Int. J. Green Nanotechnol. Phys. Chem. 1 (2010) 2, https://doi.org/10.1080/19430871003684440.

[9] M.S. Diallo, N.A. Fromer, M.S. Jhon, J. Nanoparticle Res. 15 (2013) 2044, https://doi.org/10.1007/s11051-013-2044-0.
[10] B. Nowack, T.D. Bucheli, Environ. Pollut. 150 (2007) 1, https://doi.org/10.1016/j.envpol.2007.06.006.
[11] M. Shafique, X. Luo, Materials 12 (2019) 15, https://doi.org/10.3390/ma12152493.
[12] M. Maksimović, Tecnol. 20 (2017) 40.
[13] C.L. Ventola, P T 40 (2015) 4.
[14] A.L. Romo, R. Quirós, Ther. Adv. Urol. 11 (2019).
[15] B. Malik, S. Bhattacharyya, Sci. Rep. 9 (2019) 9788, https://doi.org/10.1038/s41598-019-46078-y.
[16] L. Wang, C. Hu, L. Shao, Int. J. Nanomed. 12 (2017).
[17] Y. Xie, Y. He, P.L. Irwin, T. Jin, X. Shi, Am. Soc. Microbiol. 77 (2011) 7, https://doi.org/10.1128/AEM.02149-10.
[18] M.A. Lalabadi, A. Ehsani, B. Divband, M.A. Sani, Sci. Rep. 9 (2019), 17439, https://doi.org/10.1038/s41598-019-54025-0.
[19] G. Franci, A. Falanga, S. Galdiero, L. Palomba, M. Rai, G. Morelli, M. Galdiero, Molecules 20 (2015) 5.
[20] X. Li, S.M. Robinson, A. Gupta, K. Saha, Z. Jiang, D.F. Moyano, A. Sahar, M. A. Riley, V.M. Rotello, ACS Nano 8 (2014) 10, https://doi.org/10.1021/nn5042625.
[21] S.-S. Gabriela, F.-R. Daniela, B.-T. Helia, Int. J. Odontostomat. 10 (2016) 3.
[22] S.M. Amininezhad, A. Rezvani, M. Amouheidari, S.M. Amininejad, S. Rakhshani, Zahedan J. Res. Med. Sci. 17 (2015) 9, https://doi.org/10.17795/zjrms-1053.
[23] Y.T. Gebreslassie, H.G. Gebretnsae, Nanoscale Res. Lett. 16 (2021) 97, https://doi.org/10.1186/s11671-021-03555-6.
[24] V.K. Vidhu, D. Philip, Spectrochim. Acta, Part A 134 (2015), https://doi.org/10.1016/j.saa.2014.06.131.
[25] D.C. Sekhar, B.S. Diwakar, N. Madhavi, Nano-Struct. Nano-Obj. 19 (2019), 100374.
[26] N.M. Al-Hada, H.M. Kamari, A.A. Baqer, A.H. Shaari, E. Saion, Nanomaterials 8 (2018) 250, https://doi.org/10.3390/nano8040250.
[27] Q. Zhao, L. Ma, Q. Zhang, C. Wang, X. Xu, J. Nanomater. 850147 (2015), https://doi.org/10.1155/2015/850147.
[28] M.V. Arularasu, M. Anbarasu, S. Poovaragan, R. Sundaram, K. Kanimozhi, C. M. Magdalane, M. Maaza, J. Nanosci. Nanotechnol. 18 (2018) 5, https://doi.org/10.1166/jnn.2018.14658.
[29] M.A.M. Akhir, K. Mohamed, H.L. Lee, S.A. Rezan, Procedia Chem. 19 (2016), https://doi.org/10.1016/j.proche.2016.03.148.
[30] C.A. Ibarguen, A. Mosquera, R. Parra, M.S. Castro, J.E. Rodríguez-Páez, Mater. Chem. Phys. 101 (2007) 433, https://doi.org/10.1016/j.matchemphys.2006.08.003.
[31] M. Azis, S.S. Abbas, W.R.W. Baharom, Mater. Lett. 91 (2013) 31, https://doi.org/10.1016/j.matlet.2012.09.079.
[32] A.D. Bhagwat, S.S. Sawant, B.G. Ankamwar, C.M. Mahajan, J. Nano El. Phys. 7 (2015) 4.
[33] S. Mukherjee, C.R. Patra, Future Sci. OA 3 (2017) 3.
[34] S. Iravani, H. Korbekandi, S.V. Mirmohammadi, B. Zolfaghari, Res. Pharm. Sci. 9 (2014) 6.
[35] M. Dell'Aglio, G. Gaudiuso, O.D. Pascale, A.D. Giacomo, Appl. Surf. Sci. 348 (2015), https://doi.org/10.1016/j.apsusc.2015.01.082.
[36] T.A. Labutin, V.N. Lednev, A.A. Ilyin, A.M. Popov, J. Anal. At. Spect. 1 (2016), https://doi.org/10.1039/C5JA00301F.
[37] X. Lia, Y. Guan, Nanotech. Precision Eng. 3 (2020) 3.
[38] M. A. Gondal, Q. A. Drmosh, T. A. Saleh, Appl. Surf. Sci. 256, 7067 https://doi.org/10.1016/j.apsusc.2010.05.027.
[39] A. Qona'ah, I. Nurhasanah, A. Khumaeni, J. Nano Res. 68 (2021), https://doi.org/10.4028/www.scientific.net/JNanoR.68.114.
[40] P.S. Bakshia, D. Selvakumara, K. Kadirvelub, N.S. Kumara, Int. J. Biol. Macromol. 150 (2019), https://doi.org/10.1016/j.ijbiomac.2019.10.113.
[41] D.E.-A. Komi, M.R. Hamblin, Int. J. Adv. Res. 4 (2016) 3.
[42] T.T.V. Phan, D.T. Phan, X.T. Cao, T.-C. Huynh, J. Oh, Nanomaterials 11 (2021) 273, https://doi.org/10.3390/nano11020273.
[43] M. Ottonelli, S. Zappia, A. Demartini, M. Alloisio, Nanomaterials 10 (2020) 2, https://doi.org/10.3390/nano10020224.
[44] D.K. Naser, A.K. Abbas, K.A. Aadim, Iraqi J. Sci. 61 (2020) 10, https://doi.org/10.24996/ijs.2020.61.10.13.
[45] R.A. Ismail, S. Erten-Ela, A.K. Ali, C. Yavuz, K.I. Hassoon, Silicon (2020), https://doi.org/10.1007/s12633-020-00676-y.
[46] D.G. Capco, Y. Chen, Nanomaterial : Impacts on Cell Biology and Medicine, Springer, Dordrecht, 2014, pp. 19–43, https://doi.org/10.1007/978-94-017-8739-0.
[47] S. Mukherji, S. Bharti, G. Shukla, S. Mukherji, Phys. Sci. Rev. (2018), https://doi.org/10.1515/psr-2017-0082, 20170082.
[48] N.Z.A. Naharuddin, A.R. Sadrolhosseini, M.H.A. Bakar, N. Tamchek, M.A. Mahdi, Opt. Mater. Express 10 (2020) 2.
[49] F. Mafuné, Y. Takeda, J.-y. Kohno, T. Kondow, J. Phys. Chem. B 104 (2000) 39, https://doi.org/10.1021/jp001803b.
[50] M. Li, Q. Lu, Z. Wang, Int. J. Nanosci. 5 (2006) 2.
[51] G. Bajaj, R. Soni, Appl. Phys. A 97 (2009) 2, https://doi.org/10.1007/s00339-009-5248-5.
[52] P. Liu, W. Cai, H. Zeng, J. Phys. Chem. C 11 (2008) 9.
[53] A. Riahi, S. Khamlich, M. Balghouthi, T. Khamliche, T.B. Doyle, W. Dimassi, A. Guizani, M. Maaza, J. Mol. Liq. 304 (2020), 112694, https://doi.org/10.1016/j.molliq.2020.112694.
[54] R. Torres-Mendieta, R. Mandragon, V. Puerto-Belda, O. Mendoza-Yero, J. Lancis, J. E. Julia, G.G. Minguez-Vega, Europ. J. Chem. Phys. and Phys. Chem. (2006), https://doi.org/10.1063/1.4984420.
[55] G.A. López-Muñoz, J.A. Pescador-Rojas, J. Ortega-Lopez, J.S. Salazar, J. A. Balderas-Lopez, Nanoscale Res. Lett. 7 (2012) 423, https://doi.org/10.1186/1556-276X-7-423.
[56] R.C. Abruzzi, B.A. Dedavid, M.J.R. Pires, Cerâmica 61 (2015) 359, https://doi.org/10.1590/0366-69132015613591919.
[57] M. Kooti, S. Gharineh, M. Mehrkhah, A. Shaker, H. Motamedi, J. Chem. Eng. 259 (2015), https://doi.org/10.1016/j.cej.2014.07.139.
[58] G. Subbiahdoss, S. Sharifi, D.W. Grijpma, S. Laurent, H.C.V.D. Mei, M. Mahmoudi, H.J. Busscher, Acta Biomater. 8 (2012) 6, https://doi.org/10.1016/j.actbio.2012.03.002.
[59] P. Kamaraj, R. Vennila, M. Arthanareeswari, S. Devikala, World J. Pharm. Pharmaceut. Sci. 3 (2014) 9.

Characteristics of tin oxide nanoparticles produced by pulsed laser ablation technique in various concentrations of chitosan liquid and their potential application as an antibacterial agent

ORIGINALITY REPORT

11%	8%	7%	0%
SIMILARITY INDEX	INTERNET SOURCES	PUBLICATIONS	STUDENT PAPERS

PRIMARY SOURCES

1	Kooti, M., S. Gharineh, M. Mehrkhah, A. Shaker, and H. Motamedi. "Preparation and antibacterial activity of CoFe2O4/SiO2/Ag composite impregnated with streptomycin", Chemical Engineering Journal, 2015. Publication	1%
2	link.springer.com Internet Source	1%
3	repository.futminna.edu.ng:8080 Internet Source	1%
4	Vidhu, V.K., and Daizy Philip. "Phytosynthesis and applications of bioactive SnO2 nanoparticles", Materials Characterization, 2015. Publication	1%
5	pdfs.semanticscholar.org Internet Source	1%

6	P. Jeyakumar. "Effect of Mepiquat Chloride on Certain Physiological and Yield Characteristics of Groundnut (Arachis hypogaea L.)", Journal of Agronomy and Crop Science, 5/1996 Publication	1 %
7	hdl.handle.net Internet Source	1 %
8	www.ncbi.nlm.nih.gov Internet Source	1 %
9	pubs.rsc.org Internet Source	<1 %
10	Submitted to Universiti Kebangsaan Malaysia Student Paper	<1 %
11	ourspace.uregina.ca Internet Source	<1 %
12	Chrys. O. Chikere, Nadimul Haque Faisal, Paul Kong-Thoo-Lin, Carlos Fernandez. "Interaction between Amorphous Zirconia Nanoparticles and Graphite: Electrochemical Applications for Gallic Acid Sensing Using Carbon Paste Electrodes in Wine", Nanomaterials, 2020 Publication	<1 %
13	soar-ir.repo.nii.ac.jp Internet Source	<1 %
14	www.degruyter.com Internet Source	<1 %

15	www.mdpi.com Internet Source	<1 %
16	Akbar, Ali, and Anil Kumar Anal. "Zinc oxide nanoparticles loaded active packaging, a challenge study against Salmonella typhimurium and Staphylococcus aureus in ready-to-eat poultry meat", Food Control, 2014. Publication	<1 %
17	Hinojal Zazo, Carmen G. Millán, Clara I. Colino, José M. Lanao. "Applications of Metallic Nanoparticles in Antimicrobial Therapy", Elsevier BV, 2017 Publication	<1 %
18	A. L. Stroyuk. "Photochemical formation of semiconducting nanostructures", Theoretical and Experimental Chemistry, 07/2008 Publication	<1 %
19	Athanassiou, C.G.. "Evaluation of two new diatomaceous earth formulations, enhanced with abamectin and bitterbarkomycin, against four stored-grain beetle species", Journal of Stored Products Research, 2007 Publication	<1 %
20	etheses.saurashtrauniversity.edu Internet Source	<1 %
	nottingham-repository.worktribe.com	

21	Internet Source	<1%
22	www.patents.com Internet Source	<1%
23	Gaber, A., A.Y. Abdel-Latief, M.A. Abdel-Rahim, and Mahmoud N. Abdel-Salam. "Thermally induced structural changes and optical properties of tin dioxide nanoparticles synthesized by a conventional precipitation method", Materials Science in Semiconductor Processing, 2013. Publication	<1%
24	Mohana Priya Subramaniam, Geetha Arunachalam, Ramamurthi Kandasamy, Pandiyarasan Veluswamy, Ikeda Hiroya. "Effect of pH and annealing temperature on the properties of tin oxide nanoparticles prepared by sol–gel method", Journal of Materials Science: Materials in Electronics, 2017 Publication	<1%
25	Vincenzo Amendola, David Amans, Yoshie Ishikawa, Naoto Koshizaki et al. "Room‐temperature laser synthesis in liquid of oxide, metal‐oxide core‐shells and doped oxide nanoparticles", Chemistry – A European Journal, 2020 Publication	<1%

26	etheses.whiterose.ac.uk Internet Source	<1 %
27	mdpi-res.com Internet Source	<1 %
28	onlinelibrary.wiley.com Internet Source	<1 %
29	publish.kne-publishing.com Internet Source	<1 %
30	scholarscompass.vcu.edu Internet Source	<1 %
31	www.freepatentsonline.com Internet Source	<1 %
32	www.ijpam.eu Internet Source	<1 %
33	www.nature.com Internet Source	<1 %
34	www.pertanika.upm.edu.my Internet Source	<1 %
35	www.science.gov Internet Source	<1 %
36	Elena Vetchinkina, Ekaterina Loshchinina, Maria Kupryashina, Andrey Burov, Valentina Nikitina. "Shape and Size Diversity of Gold, Silver, Selenium, and Silica Nanoparticles	<1 %

Prepared by Green Synthesis Using Fungi and Bacteria", Industrial & Engineering Chemistry Research, 2019
Publication

37	M. Tchaplyguine, C. Wright, A. Shavorskiy, S. Zhu et al. "Tin-oxide nanoparticles deposited from a beam: what happens to the composition?", Physical Chemistry Chemical Physics, 2019 Publication	<1 %
38	Mat Don Mashitah, Yen San Chan, Jeevanandam Jason. "Antimicrobial properties of nanobiomaterials and the mechanism", Elsevier BV, 2016 Publication	<1 %
39	Mostafa M. Amini, Ezzatollah Najafi, Behzad Karami, Hamidreza Khavasi. " Synthesis and characterization of a new organotin(IV) complex as a new precursor for preparation SnO nanoparticles ", Inorganic and Nano-Metal Chemistry, 2016 Publication	<1 %

Exclude quotes Off
Exclude bibliography On
Exclude matches Off

Characteristics of tin oxide nanoparticles produced by pulsed laser ablation technique in various concentrations of chitosan liquid and their potential application as an antibacterial agent

GRADEMARK REPORT

FINAL GRADE

/0

GENERAL COMMENTS

Instructor

PAGE 1

PAGE 2

PAGE 3

PAGE 4

PAGE 5

PAGE 6